

Molecular Logic Gates Based on Pentacyanoferrate Complexes: From Simple Gates to Three-Dimensional Logic Systems

Konrad Szaciłowski*^[a]

Abstract: The article presents new aspects of reactivity of two pentacyanoferrates: $[\text{Fe}(\text{CN})_5\text{NO}]^{2-}$ and $[\text{Fe}(\text{CN})_5\text{N}(\text{O})\text{SR}]^{3-}$. The dependence of thermodynamic functions on cations was found for the reaction between nitroprusside and thiolate. The thermodynamic data are interpreted in terms of ion pairing and changes in the solvation shell of the cations. It was found that the reaction enthalpies and entropies depend strongly on the cation

radius. The reaction volume in turn is strongly affected by the structure and properties of the hydration shell. Careful data analysis allowed the contribution of partial cation dehydration to the total reaction volume to be determined. The experimental results were

Keywords: cations • molecular devices • molecular logic gates • pentacyanoferrates • photochemistry

also interpreted in terms of chemical logic gates. Complex logic systems were built from a number of cells containing a switching compound arranged in different geometric patterns. Increasing the dimensionality of these arrangements leads to really complex logic systems containing up to 20 AND and OR logic gates. The system is capable of processing up to 16 bits of input data.

Introduction

Rapid development of different electronic devices was initiated by the discovery of the semiconductor-based switch—a transistor in 1948 by J. Bardeen, W. H. Brattain and W. B. Shockley.^[1,2] All electronic devices have been based on semiconductor components ever since. Growing demand for bigger memories and faster processors requires smaller and smaller transistors and other components. According to Moore's law, the complexity of integrated semiconductor devices doubles every 18 months.^[3] Increasing the complexity and degree of integration of electronic circuits are achieved by miniaturisation of semiconductor structures. With decreasing dimensions of electronic elements, tunnelling currents through the insulation barrier increase and the breakdown voltage of the insulator decreases.^[4] Soon the integration scale of electronic components will reach its physical limits and further acceleration will not be possible.^[5] The only solution to the crisis is the application of single molecules and molecular systems for data acquisition, storage, transfer and processing.^[6]


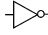


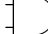

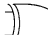

There are a multitude of chemical systems capable of digital-data processing. They are based on fullerenes,^[7] carbon

nanotubes,^[8–10] DNA,^[11–14] Aviram–Ratner type devices^[15–17] and Tour wires.^[17–19] All these systems, except DNA, are based however, on the classical electronics paradigm. Logic gates and switches are in principle based on the same phenomena as semiconductor devices. Chemical logic gates present another approach. These systems consist of molecules that can exist in at least two different states (isomers, rotamers, etc.) and there are defined physical or chemical stimuli capable of switching the system from one state to the other (e.g., light, redox potential, temperature, pressure, pH, metal ions, etc.).^[20–34]

The principles of the operation of chemical logic gates are identical to those of electronic logic gates. The input and output signals may have only two values: 0 (OFF, FALSE) or 1 (ON, TRUE). The output signal is a Boolean function of the input signals. The basic logic gates are YES, NOT, OR, NOR, AND, NAND, EX-OR and EX-NOR. The truth tables and symbols of these gates are presented in Table 1. In the case of electronic devices, inputs and outputs are electric signals, typically logical 0 corresponds to the potential of 0.0–0.4 V and logical 1 to 2.4–3.3 V versus the earth potential. In chemical systems there is a much larger variety of different signals and logical values may be attributed arbitrarily, for example, logical 1 may be attributed to high absorbance or to high transmittance of the solution, low or high pH, and so on. Usually in one chemical system, different attribution of logic variables results in different logic functions.^[24]

[a] Dr. K. Szaciłowski
Faculty of Chemistry, Jagiellonian University
Ingardena 3, 30-060 Kraków (Poland)
Fax: (+48) 12-6335392
E-mail: szacilow@chemia.uj.edu.pl

Table 1. Symbols and truth tables of basic logic gates.

Logic function	Symbol	Truth table			
YES		A	X	X'	
NOT		0	0	1	
		1	1	0	
OR		A	B	X	X'
		0	0	0	1
NOR		0	1	1	0
		1	0	1	0
		1	1	1	0
AND		A	B	X	X'
		0	0	0	1
NAND		0	1	0	1
		1	0	0	1
		1	1	1	0
EX-OR		A	B	X	X'
		0	0	0	1
EX-NOR		0	1	1	0
		1	0	1	0
		1	1	0	1

Usually the chemical logic systems are based on extremely complicated supramolecular complexes, such as Balzani's and Stoddart's "molecular meccano"^[20–23] systems (rotaxanes, catenanes and dendrimers) or large organic ligands encompassing receptor sites and chromo- or fluorophores, like de Silva's systems.^[25–27,35] However, there are other systems much simpler from a chemical point of view, but their logic structure is even more complicated compared with previously mentioned systems. One of these systems, described recently by F. Raymo and co-workers,^[28–34] consists of one

Abstract in Polish: Niniejszy artykuł przedstawia nowe aspekty reaktywności dwóch pentacyjanożelazianów: $[\text{Fe}(\text{CN})_5\text{NO}]^{2-}$ i $[\text{Fe}(\text{CN})_5\text{N}(\text{O})\text{SR}]^{3-}$. Określono zależność pomiędzy funkcjami termodynamicznymi reakcji pomiędzy anionem nitroprusydku a anionami tiolanowymi od kationów obecnych w środowisku reakcji. Dane termodynamiczne zostały zinterpretowane w oparciu o prosty model elektrostatyczny tworzenia par jonowych oraz zmiany w otoczkach solwacyjnych kationów. Stwierdzono, że entalpie molowe badanej reakcji silnie zależą od promienia kationu, a objętość molowa reakcji jest głównie związana ze strukturą i właściwościami otoczki solwacyjnej. Szczegółowa analiza danych pozwoliła na obliczenie udziału częściowej desolvatacji kationu w całkowitej objętości reakcji. Dane eksperymentalne zostały także wykorzystane do stworzenia szeregu modeli molekularnych układów logicznych. Złożone układy logiczne zostały zbudowane w oparciu o różne zestawy kuwet zawierających roztwory związków o właściwościach przełączników molekularnych. Wraz z rosnącą liczbą wymiarów geometrycznych tych zestawów zauważono rosnący stopień złożoności realizowanych funkcji logicznych. Największy badany układ zawiera 20 bramek typu AND i OR. Układ ten umożliwia jednoczesne przetwarzanie 16 bitów informacji.

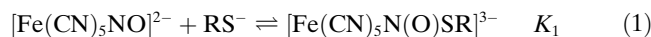
photochromic system (spiropyran/merocyanine), simple indicators (like methyl orange) and fluorescent aromatic hydrocarbons. Despite chemical simplicity, the system is capable of complex logic operations and even emulates the behaviour of a one-bit memory.

One of the most challenging problems of molecular logic systems is data transmission between individual components to form an array of gates. This issue is trivial in the case of traditional electronics, but "wiring" of chemical logic gates is a serious problem. One of the most exciting logic networks was recently presented by Stojanovic and Stefanovic.^[14] The DNA-based chemical automaton plays tic-tac-toe and never loses. In this system however, direct data flow between the elements of the array does not take place. This problem of information transfer between the chemical logic gates was recently solved by F. Raymo using photoinduced proton transfer reactions^[28,31] to connect different switching molecules or optical connections in a one-dimensional array of cells.^[32,33] A similar approach was also used by V. Balzani et al. in a chemical system mimicking some properties of neurons.^[36] Another possibility was described by Showalter et al.: the propagation of a chemical wave in an excitable medium provides both logic operations and information transfer between different parts of the logic circuit.^[37] This paper deals with several molecular logic systems of increasing complexity and presents a simple solution to data transmission using visible light.

Results and Discussion

Thermal reactivity: Cyanoferrates are widely used as chemosensors, electrocatalysts, ion exchangers and molecular magnets. Their exceptional chemical and optical properties, together with a rich reactivity, make them ideal candidates for molecular logic gates. One of the most widely studied member of the family is pentacyanonitrosylferrate(2−), usually called nitroprusside. For many years it has been studied because of its physiological reactivity and medical applications,^[38–42] but recently it has been applied as a building block in supramolecular networks,^[43,44] magnetic switches^[45] and organic conductors.^[46–50]

In alkaline solution nitroprusside reacts with thiolates yielding a dark-red nitrosothiol complex of the type $[\text{Fe}(\text{CN})_5\text{N}(\text{O})\text{SR}]^{3-}$, as shown in the equilibrium in Equation (1):^[51]



In most cases, the product of the reaction is thermally unstable and undergoes an intramolecular redox reaction yielding the $[\text{Fe}(\text{CN})_5\text{NO}]^{3-}$ complex and disulfide as main products.^[51,52] If the thiol molecule contains electron-withdrawing groups, the stability increases: the most stable is the complex with mercaptosuccinate.^[51] Electronic spectra of the $[\text{Fe}(\text{CN})_5\text{NO}]^{2-}$ and $[\text{Fe}(\text{CN})_5\text{N}(\text{O})\text{SR}]^{3-}$ complexes are shown in Figure 1a and 1b, respectively.

The equilibrium [Eq. (1)] is extremely sensitive to different stimuli, such as pH, cation type and concentration, tem-

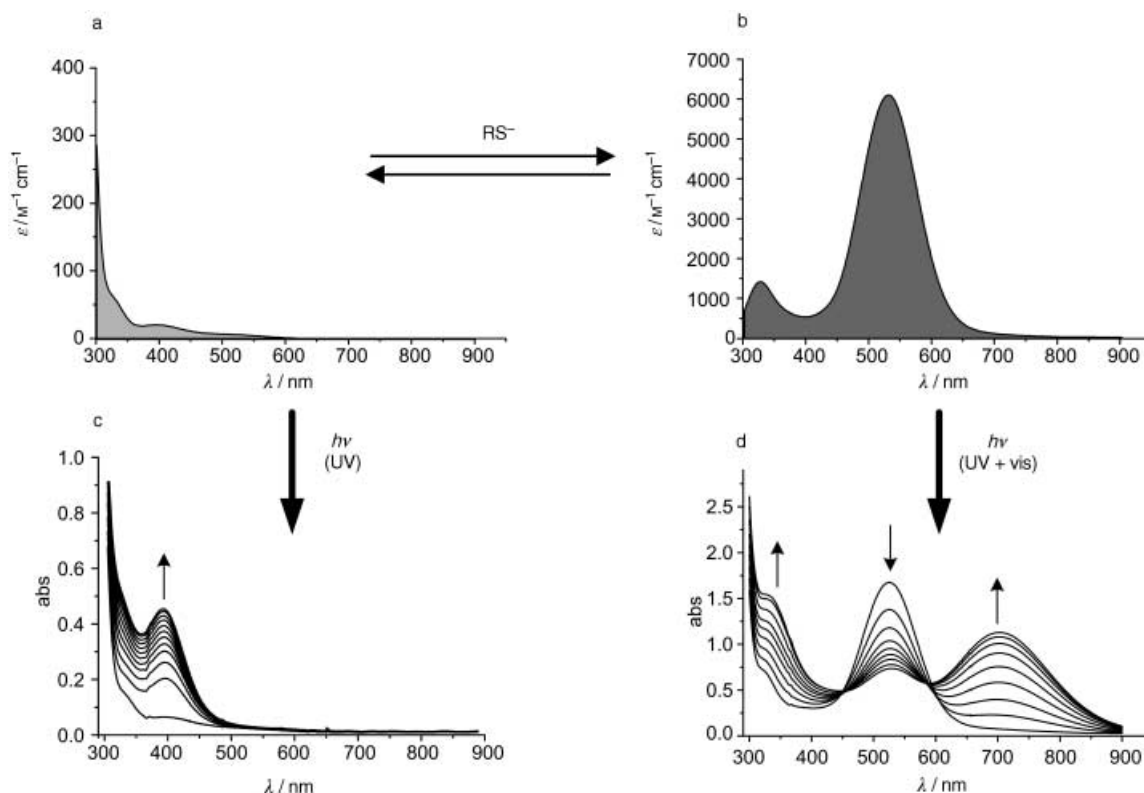


Figure 1. The versatile photochemistry of the nitroprusside-thiolate system: absorption spectra of the a) $[\text{Fe}(\text{CN})_5\text{NO}]^{2-}$ and b) $[\text{Fe}(\text{CN})_5\text{N}(\text{O})\text{SR}]^{3-}$ complexes; spectral changes recorded during c) 365 nm irradiation of $[\text{Fe}(\text{CN})_5\text{NO}]^{2-}$ (2.5×10^{-3} M, pH 10, time interval 60 s) and d) 546 nm irradiation of $[\text{Fe}(\text{CN})_5\text{NO}]^{2-}$ with mercaptosuccinate (1.25×10^{-2} M, pH 10, time interval 60 s).

perature, pressure and light.^[24,51,53–56] Increasing the pH shifts the equilibrium to the right, while decreasing the pH shifts it to the left. The pH-dependence profile (Figure 2a) is almost identical to the titration curve of thiols. The effect of the ionic environment is more complex. Increasing the ionic strength at constant cation concentration shifts the equilibrium [Eq. (1)] to the left, whereas increasing the cation concentration shifts it to the right (Figure 2b). Increasing the ionic strength at constant cation concentration can only be achieved by exchanging monovalent anions with higher-charged species, which can compete more efficiently with nitroprusside in ion-pair formation. Moreover, increasing the ionic strength decreases the mean-activity coefficients according to the Debye–Hückel equation.

Increasing the cation concentration also increases the ionic strength of the reaction medium, but increasing the number of cations facilitates ion-pair formation. When the cation effect (ion-pair formation) prevails over the ionic-strength effect (Debye–Hückel contribution), a significant increase of the equilibrium constant K_1 is observed; large cations that form only very weak ion pairs do not stabilise the $[\text{Fe}(\text{CN})_5\text{N}(\text{O})\text{SR}]^{3-}$ complex because the ionic-strength effect dominates over the cation effect.

The crucial role played in the specific-cation effect is the Coulombic interaction between the nitroprusside anion and cations.^[51,56] The smaller the cation, the larger the equilibrium constant for Equation (1). The dependence of the equi-

librium constant K_1 on the radius of the cation is approximately linear [Eq. (2), cf. Figure 2c],

$$\Delta G \propto \ln K_1 \propto \frac{z_1 z_2}{r_1 + r_2} \quad (2)$$

in which z_1 and z_2 are the charges, and r_1 and r_2 the radii of the cation and nitroprusside, respectively. The dependence on organic cations is linear indicating that the electrostatic interaction is the principal one in this case. Alkali-metal cations show small deviations from linearity, which is the consequence of other interactions, such as polarisability, specific interactions of cations with lone pairs of CN^- ligands, or changes in the structure of the hydration shell of the cation upon ion-pair formation (vide infra).

Influence of temperature and pressure on the equilibrium:

For all the cations, increasing the temperature shifts the equilibrium [Eq. (1)] to the left. The process is fully reversible and decreasing the temperature restores the initial concentration of the $[\text{Fe}(\text{CN})_5\text{N}(\text{O})\text{SR}]^{3-}$ complex. This behaviour produces significant negative values of enthalpy for Equation (1). Table 2 collates the values of the thermodynamic functions for the equilibrium [Eq. (1)] in the case of different inorganic and organic cations.

The dependence of the ΔH values for Equation (1) on the cation type is consistent with previous observations.^[51] Alkali-metal cations favour the formation of the $[\text{Fe}(\text{CN})_5\text{N}(\text{O})\text{SR}]^{3-}$ complex.

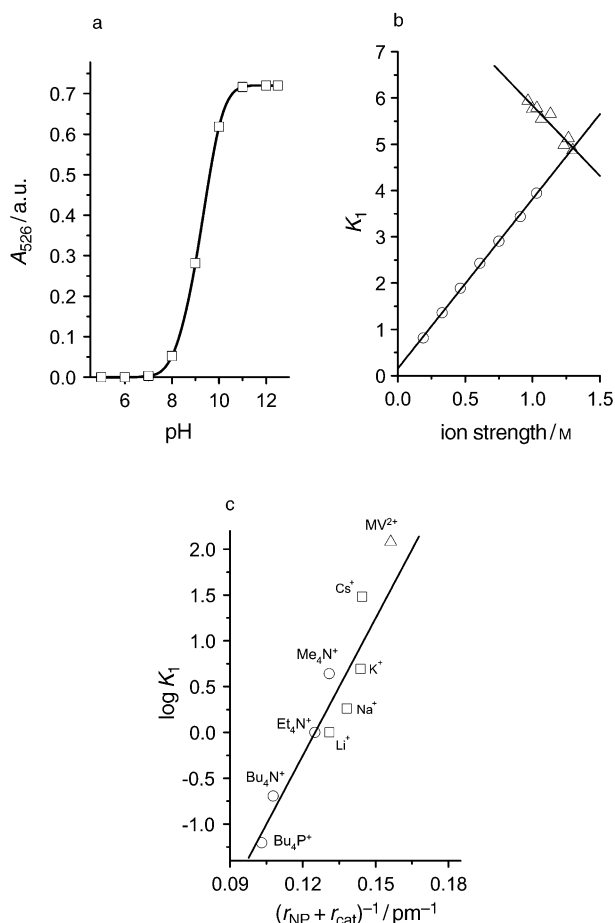


Figure 2. The dependence of K_1 on different chemical stimuli: a) absorption changes in TRIS buffer containing potassium chloride (0.2 M); b) the influence of sodium chloride concentration (\circ) and changes in ionic strength at constant sodium concentration (Δ); c) the influence of the cations on the equilibrium in Equation (1), the cation concentration is 0.2 M in each case.

Table 2. Thermodynamic functions for the formation of the $[\text{Fe}(\text{CN})_5\text{-N}(\text{O})\text{SR}]^{3-}$ complex in the presence of different cations and hydrated radii of cations.

Cation	Radius[pm] ^[a]	ΔH [kJ mol ⁻¹]	ΔS [J ⁻¹ mol ⁻¹ K ⁻¹]	ΔV [cm ⁻³ mol ⁻¹]
Li ⁺	307	-31.1	-89.5	-14.9
Na ⁺	292	-24.1	-62.7	-14.2
K ⁺	279	-29.7	-77.0	-13.5
Cs ⁺	277	-45.9	-125.3	-11.3
Me ₄ N ⁺	298	-72.5	-226.2	-15.5
Et ₄ N ⁺	320	-43.4	-136.6	-20.4
Pr ₄ N ⁺	362	-21.8	-71.0	-13.0
Bu ₄ N ⁺	396	-12.1	-38.6	-7.9

[a] Hydrated or unhydrated, calculated according to data from ref. [57].

$\text{N}(\text{O})\text{SR}]^{3-}$ complex. The largest energetic effect is observed for the caesium cation ($-45.9 \text{ kJ mol}^{-1}$, cf. Table 2) and the smallest for sodium ($-24.1 \text{ kJ mol}^{-1}$). Contrary to previous reports, the lithium cation gives a slightly larger effect ($-31.1 \text{ kJ mol}^{-1}$) than sodium. It is justified by the exceptionally high affinity of lithium towards hydration.^[57] Caesium has the smallest hydrated radius among all of the alkali-

metal cations, so the highest energetic effect supports the electrostatic model. The behaviour of tetraalkylammonium cations fits very well to the simple electrostatic model. The smallest cation (Me_4N^+) exhibits the largest affinity toward ion-pair formation, while the largest cation (Bu_4N^+), the smallest affinity.

Reaction entropies are negative in all the cases under study, which is consistent with the associative mechanism of Equation (1). In each group (alkali metals and tetraalkylammonium) the most negative values were measured for the cations with the highest affinity towards nitroprusside: caesium and Me_4N^+ . The associative character of the reaction [Eq. (1)] is also supported by significantly negative reaction volumes. There are, however, at least three components contributing to the reaction volume that should be taken into account [Eq. (3)]: electrostriction of the solvent molecules in the vicinity of the reacting ions (V_{el}), changes in the hydration number of the hydrated cations (V_{hydr}) and the intrinsic reaction volume (V_{intr}).^[58]

$$V_{\text{total}} = V_{\text{el}} + V_{\text{hydr}} + V_{\text{intr}} \quad (3)$$

The dependence of the total reaction volume (V_{total}) on the ionic radius of the cations (Figure 3) shows that the cat-

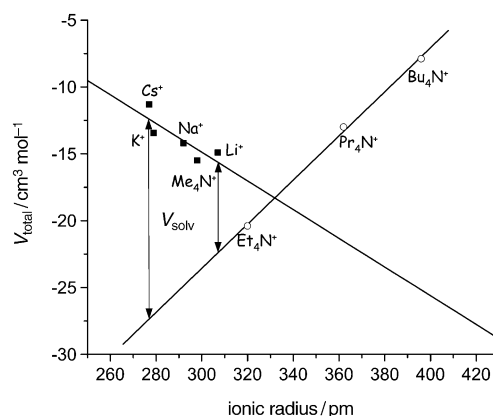
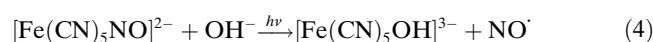


Figure 3. The correlation between the ionic radius of hydrated (\blacksquare) and unhydrated (\circ) cations and the reaction volume V_{total} . Vertical arrows show the estimated values of the solvation contribution (V_{solv}) to the total reaction volume.

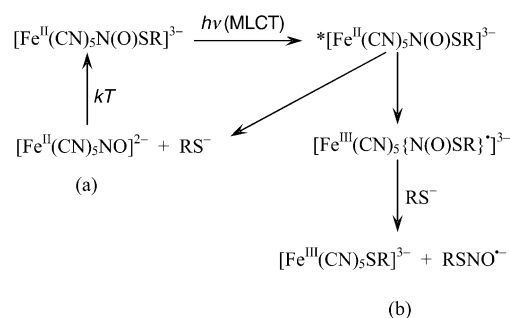
ions can be divided into two different groups. This division is consistent with the hydration of the cations. The reaction volume for hydrated cations (Li^+ , Na^+ , K^+ , Cs^+ , Me_4N^+) decreases with increasing ionic radius, but decreases for unhydrated ions (Et_4N^+ , Pr_4N^+ , Bu_4N^+). The intrinsic (V_{intr}) and electrostriction (V_{el}) values should not depend dramatically on the hydration of the cations. The only component that plays an important role here is the component associated with changes in the hydration sphere (V_{hydr}). Its value is the highest for caesium ($\sim 15 \text{ cm}^3 \text{ mol}^{-1}$) and the smallest for lithium ($\sim 6 \text{ cm}^3 \text{ mol}^{-1}$, vertical arrows on Figure 3). It is fully explained by the difference in hydration of the cations. Cae-

sium binds water molecules weakly and upon ion-pair formation they are easily displaced from the hydration shell. Lithium in turn binds water molecules strongly, they are not easily removed and the V_{hydr} component is small.^[59] These results are supported by electrospray ionization mass spectrometry (ESIMS) and ^{13}C NMR studies, proving the importance of cation hydration in the reaction between thiolates and nitroprusside.^[56]

Photochemistry: Both components of the equilibrium are photosensitive. Nitroprusside undergoes photooxidative substitution upon irradiation with light within the range of 313–500 nm. The products are nitric oxide and the $[\text{Fe}(\text{CN})_5\text{OH}]^{3-}$ complex ($\lambda_{\text{max}}=392$ nm) as shown in Equation (4).^[60–63] Spectral changes during the process are shown in Figure 1c.



The photochemistry of the $[\text{Fe}(\text{CN})_5\text{N}(\text{O})\text{SR}]^{3-}$ complex is more complicated. Two main pathways involve photodissociation (Scheme 1a) and photooxidative-substitution (Scheme 1b) modes. The metal-to-ligand charge transfer



Scheme 1. The mechanism of the photochemical reaction for the $[\text{Fe}(\text{CN})_5\text{N}(\text{O})\text{SR}]^{3-}$ complex upon excitation with visible light.

(MLCT) excitation populates the antibonding orbital of the RSNO ligand, which results in the weakening of the S–N bond and dissociation of the complex.^[54,55] The same process also results in the reduction of the ligand to the nitrosothiyl radical, which is a very poor ligand and is easily substituted by an excess of thiolate. The resulting $[\text{Fe}(\text{CN})_5\text{SR}]^{3-}$ complex is characterised by a strong LMCT absorption band at 700 nm ($\epsilon=2800\text{ M}^{-1}\text{ cm}^{-1}$).^[54,55] The RSNO^- radical undergoes numerous reactions yielding RSNO and $[\text{Fe}(\text{SR})_2(\text{NO})_2]^-$.^[54,55] Spectral changes recorded during irradiation are presented in Figure 1d.

Logic systems based on pentacyanoferrate complexes: Any chemical system that can exist in two different states with significantly different spectroscopic properties and reactivity may be used to build the chemical logic gate. The system consisting of two pentacyanoferrates in equilibrium is a very good model for molecular logic gates. All the stimuli shifting the equilibrium in Equation (1) (pH, cations, temperature and pressure) can be used to encode input information,

while absorbance and transmittance at 520 nm and generation of photoproducts can be used as an output.^[24]

Zero-dimensional system: As mentioned before, the equilibrium in Equation (1) is very sensitive to different physical and chemical stimuli. The most important, and also the easiest to control, are pH and cation concentration (for example K^+). Optical properties (absorbance at 520 nm) of the solution containing nitroprusside and mercaptosuccinate strongly depend on pH and $[\text{K}^+]$. When both are low, the equilibrium [Eq. (1)] is shifted completely to the left; that is, no $[\text{Fe}(\text{CN})_5\text{N}(\text{O})\text{SR}]^{3-}$ complex is formed. Addition of base (to achieve a pH of 10) or introduction of an electrolyte forming stable ion pairs with the $[\text{Fe}(\text{CN})_5\text{NO}]^{2-}$ complex does not change the equilibrium, and the solution remains virtually colourless. When both pH and $[\text{K}^+]$ are high, the $[\text{Fe}(\text{CN})_5\text{N}(\text{O})\text{SR}]^{3-}$ complex is formed and the solution turns red.

This behaviour of the system can be described in terms of Boolean logic as an AND gate. The pH and $[\text{K}^+]$ can be treated as input signals and the absorbance at 520 nm as the output (Table 3). Low pH and $[\text{K}^+]$ values can be attributed

Table 3. Assignment of logic values to the input and output signals of a simple chemical logic gate based on the pentacyanoferrate complex.

Physicochemical parameters			Logical parameters		
pH	$[\text{K}^+]$	Abs @ 520 nm	Input I	Input II	Output
low	low	low	0	0	0
low	high	low	0	1	0
high	low	low	1	0	0
high	high	high	1	1	1

to logical 0 (FALSE) and high values of these parameters to logical 1 (TRUE). The high absorbance at 520 nm can be attributed to logic 1 and low absorbance to logic 0. The same can be done with transmittance of the solution. If transmittance is taken as an output, the system behaves like a NAND gate (a combination of AND and NOT, cf. Table 1). This is directly related to the positive and negative logic in semiconductor-based systems.

The behaviour of more complex logic systems can be reproduced with the studied chemical system when the number of input and output parameters is increased. Changes in temperature and pressure, and induction of photochemical processes may lead to different logic systems, not only digital, but also analogue. The simplest device in this category is an AND gate based on a photochemical reaction. Visible irradiation (at 520 nm) induces photogeneration of nitrosothiol and the Fe^{III} -thiolate complex only in the presence of a sufficient concentration of electrolyte and at the required pH.

Especially important are the systems that can perform complex logic operations and process data from multiple inputs. The easiest way to extend the operation of the chemical logic gate without substantial changes in the chemistry involved, is to increase the number of simple logic gates and provide communication between them. One spectrophotometric cell containing the switchable solution behaves as a

single AND gate, but a set of a certain number of cells arranged geometrically gives new possibilities.

One-dimensional system: The simplest logic system with real data flow between logic gates can be achieved when two or more cells containing the switching system are placed in series. The connection between logic gates can be realised using a light beam ($\lambda = 520$ nm) passing through all the cells (Figure 4a). The simplest system is that containing two identical cells.

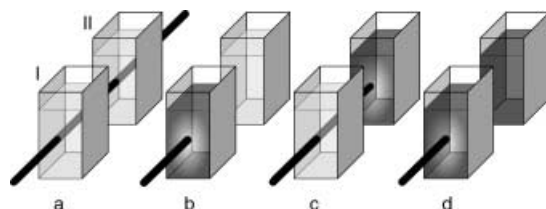


Figure 4. A schematic view of the arrangement of two absorption cells in a one-dimensional logic system. The cells on the OFF state are marked pale grey and the cells in the ON state are dark grey.

Every cell works as a single AND gate. An output signal can be attributed to absorbance (X_1) at 520 nm of the cell set and occurrence of a photochemical reaction upon visible excitation in the first (X_2) and second (X_3) cell. Input signals were assigned to pH and $[K^+]$ (or another alkali-metal cation) in every cell. The truth table of the system is shown in Table 4.

Table 4. Truth table of the system consisting of two cells with the $[\text{Fe}(\text{CN})_5\text{NO}]^{2-} \rightarrow [\text{Fe}(\text{CN})_5\text{N}(\text{O})\text{SR}]^{3-}$ system. AND_I and AND_{II} define logic states of individual cells, inputs a and b refer to the pH and $[K^+]$, respectively.

Cell I		Cell II		Output		
Inputs a, b	AND_I	Inputs c, d	AND_{II}	X_1	X_2	X_3
0 0		0 0				
0 1	0	0 1	0	1	0	0
1 0		1 0				
0 0						
0 1	0	1 1	1	0	0	1
1 0						
		0 0				
1 1	1	0 1	0	0	1	0
		1 0				
1 1	1	1 1	1	0	1	0

The system has low absorbance only when both cells have low absorbance (Figure 4a), that is, when the equilibrium [Eq. (1)] is shifted to the left. High absorbance can in turn, be achieved when in at least one cell the equilibrium is shifted to the right (Figure 4b, 4c). As the logic state of any individual cell depends on two parameters (pH and $[K^+]$, (a, b) for the first and (c, d) for the second cell, respectively), the X_1 output can be described as a Boolean function of four variables [Eq. (5), Figure 5a].

$$X_1 = a \cdot b + c \cdot d \quad (5)$$

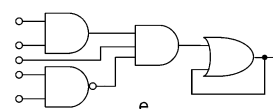
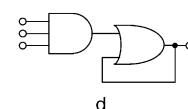
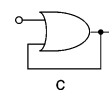
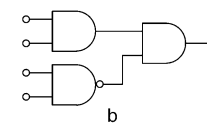
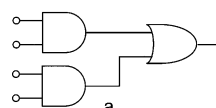


Figure 5. Electronic equivalents of the one-dimensional logic systems: a) absorption mode; b) logic circuit based on a photochemical reaction in cell II; c) one-bit memory; d) logic circuit based on a photochemical reaction in cell I with a one-bit memory; e) logic circuit based on a photochemical reaction in cell I with a one-bit memory.

A photochemical reaction, upon visible irradiation in the first cell, occurs only when the solution is in the ON state, while in the second cell a reaction occurs only when the first cell is in the OFF state and the second in the ON state [Eq. (6), Figure 5b].

$$\begin{aligned} X_2 &= a \cdot b \\ X_3 &= \overline{a \cdot b} \cdot c \cdot d \end{aligned} \quad (6)$$

Thermal stability of one of the photoproducts ($[\text{Fe}(\text{CN})_5\text{SR}]^{3-}$) implies that the system behaves like a one-bit memory cell (Figure 5c). The X_2 and X_3 output values are preserved for the period of the $[\text{Fe}(\text{CN})_5\text{SR}]^{3-}$ complex's lifetime (approximately 600 s). If visible irradiation is treated as one more input signal (ν), the X_2 will actually be the three-input AND gate (X_4), and the X_3 output will depend on five different inputs (X_5) [Eq. (7)].

$$\begin{aligned} X_4 &= a \cdot b \cdot \nu \\ X_5 &= \overline{a \cdot b} \cdot c \cdot d \cdot \nu \end{aligned} \quad (7)$$

Together with the one-bit memory, the circuitry of these systems is quite complicated (Figure 5d, 5e).

Two-dimensional system: The next step of increasing complexity of the computing system is achieved in the square network of cells (Figure 6a). The simplest system of this kind consists of four identical switching cells placed in four edges of the square. Four light sources and four detectors ensure easy information readout. Every cell responds to the

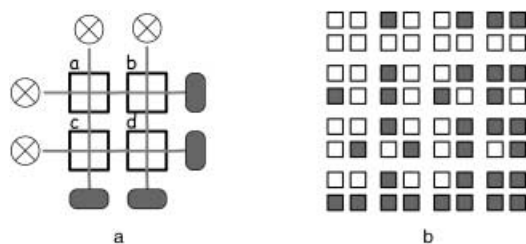


Figure 6. a) The spatial arrangement of the cells in a two-dimensional logic system; b) all possible logic states of the system.

switching by using pH and cation concentration, such as in the previous case. Four independent outputs may be associated with light absorption (or transmission) in every row and column. There are 256 different combinations ($2^8=256$) of input parameters and the system exists in 16 different states (Figure 6b). If light absorption at 520 nm is assigned to be the output parameter, the system behaves like its electric equivalent, as shown in Figure 7a. On every

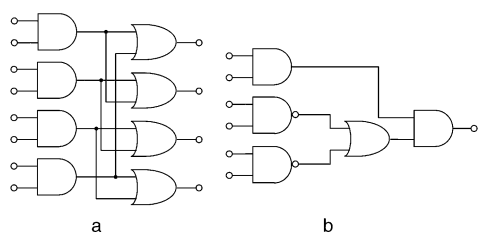


Figure 7. Electronic equivalents of the two-dimensional logic circuit: a) absorption mode; b) system based on a photochemical reaction in cell *d*.

edge, light is absorbed if at least one of the cells is in the ON state. Four edges connecting four cells correspond to four 2-input AND gates (one gate for every cell in the system) and four OR gates (one gate for every edge of the square). Additional complications can be introduced due to the photochemical reactivity of the $[\text{Fe}(\text{CN})_5\text{N}(\text{O})\text{SR}]^{3-}$ complex. There is one cell in the system that is not irradiated directly, but through other cells (see Figure 6a, cell *d*). The occurrence of a photochemical reaction in this cell depends on two factors: 1) absorbance of the solution in this cell and 2) absorption of the solutions in other cells. Cell *d* must be switched to 1 and cell *b* or *c* must be in the 0 state. It corresponds to the set of 5 logic gates connected as shown in Figure 7b. As in the previous photochemical system, the output may be additionally equipped with a one-bit memory cell. Any larger $N \times N$ matrices can be described in the same way, with a larger number of individual gates and a more complicated network of connections.

Three-dimensional system: Maximal complexity of logic behaviour can be achieved in a three-dimensional system (Figure 8). It consists of eight identical cells with a switching compound placed at the corners of the cube, 12 light sources (placed on *abcd*, *aceg* and *abef* walls of the cube) and 12 detectors (on *efgh*, *cdgh* and *bdfh* walls), and light is guided

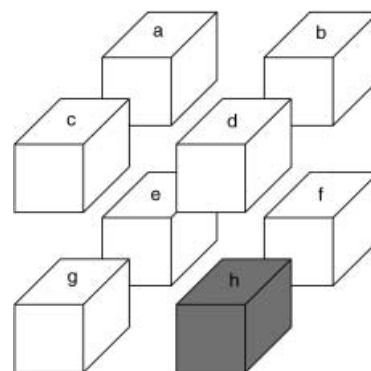


Figure 8. Schematic view of the three-dimensional logic system. Cell *h* can be irradiated only via cells *d*, *f* or *g*.

along all 12 edges. The system has 16 data inputs (8 cells with two inputs each) and 12 outputs (12 edges of the cube). The logic structure of this system is much more complicated than the previous systems. There are 65536 (2^{16}) different combinations of input parameters and 256 different sets of 12-bit outputs. Every edge of the cube, like in the previous case, works like a circuit containing two AND and one OR gate. The electronic equivalent of the system is shown in Figure 9a. The circuitry looks very complicated, but it is a set of simple components connected in parallel (cf. Figure 5a).

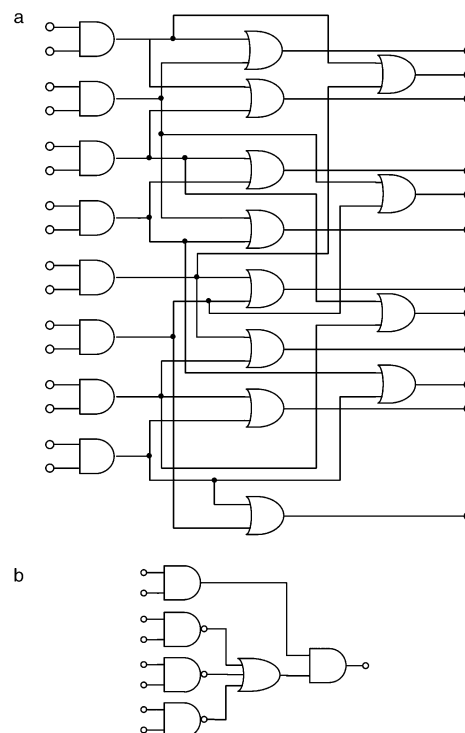


Figure 9. Electronic equivalents of the three-dimensional system: a) absorption mode; b) system based on a photochemical reaction in cell *h*.

One cell in the set (cell *h* in Figure 8) cannot be irradiated directly, instead the light beam must pass through the other cells first. Photochemical reactions induced by visible-light

irradiation can occur only when cell h is in the ON state and at least one of the cells d , f or g is in the OFF state. The electronic equivalent of this system is shown in Figure 9b. Three NAND gates correspond to three edges of the cube, which must be transparent at 520 nm (in the OFF state) in order to induce a reaction in cell h . The first AND gate depicts cell h , which must be in the ON state. The OR gate illustrates that only one “transparent” edge is enough to supply light to the cell. The last AND gate (at the output) checks if both conditions are fulfilled: cell h is illuminated and is in the ON state. As in the previous photochemical system, the output may be additionally equipped with a one-bit memory cell. The principle of operation for all the logical systems based on photochemical reactions induced by 520 nm light is identical, but the complexity increases with increasing dimensionality of the cell set, that is, the number of the NAND gates increases and is equal to the number of edges that the irradiated cell shares with others.

Larger $N \times N \times N$ arrays or other geometrical arrangements of the cells lead to increased complexity of the logic operation that can be performed with the system, but the basic principles remain unchanged.

Conclusion

The reactivity and photoreactivity of the nitroprussidethiolate system is easily modified by different physical and chemical stimuli. Ionic strength, cation type and concentration and pH, control the equilibrium [Eq. (1)]. Influence of temperature and pressure on the equilibrium is cation dependent and analysis of the thermodynamic data shows the important role of size and structure of the hydration sphere of the cation.

The irreversibility of the photochemical reaction in this system seems to be very disadvantageous. The photoproducts, however, are molecules of rich biological activity. It creates a possibility for the application in related systems, such as “tunable” or “programmable” drugs. Photogeneration of nitric oxide or S -nitrosothiols on demand has important medical implications.^[41]

All of the parameters influencing the system can be used to mimic the behaviour of logic gates. The use of only two parameters (pH and cation concentration) leads to very complex logical systems. These are the most complicated chemical logic systems ever described in the literature. The complexity of these systems can also be increased by the introduction of other control parameters, and by the application of analogue processing elements (i.e., the chemical equivalent of operational amplifiers).^[24] The degree of complexity of the different logic systems presented in this paper depends strongly on the geometrical arrangement of individual switching cells, especially for two-dimensional and three-dimensional systems. This dependence was restricted to the simplest arrangements of a given dimensionality. It is possible, however, to apply more complicated geometrical patterns and to use a larger number of switches to achieve complex computing circuits.

Experimental Section

The $[\text{Fe}(\text{CN})_5\text{N}(\text{O})\text{SR}]^{3-}$ complex was generated in situ from sodium nitroprusside and mercaptosuccinic acid.^[51] All other chemicals were of analytical purity (Aldrich). A carbonate/borate buffer of pH 10 was prepared from triply-distilled water and used in all the experiments.

UV/Vis spectra were recorded on Shimadzu UV-Vis 2100 and Hewlett-Packard HP 8463 spectrophotometers in a 1 cm quartz cell. A high-pressure mercury lamp (HBO 200) equipped with a LPS 250 power supply (Photon Technology International) was used as a light source; chosen wavelengths were selected using interference filters. High-pressure measurements were performed on the custom-built instrument described elsewhere.^[64]

Circuitry analyses was performed by using CircuitMaker 6.2 (Protel Technology Inc., USA).

Acknowledgements

The author would like to express his gratitude to Prof. Zofia Stasicka for encouragement and helpful discussions and Mr. Zygmunt Wolek for assistance during the high-pressure experiments. The work was supported by the Jagiellonian University (grant no. DBN-414/CRBW/K-VIII-23/2003).

- [1] J. Bardeen, W. Brattain, US Patent 2524035, 1948.
- [2] W. Shockley, US Patent 2569347, 1948.
- [3] G. E. Moore, *Electronics* **1965**, 38, 114.
- [4] Y. Taur, *Proc. IEEE* **1997**, 85, 486.
- [5] R. W. Keyes, *Proc. IEEE* **2001**, 89, 227.
- [6] R. F. Service, *Science* **2002**, 295, 2398.
- [7] C. Joachim, *Superlattices Microstruct.* **2000**, 28, 305.
- [8] G. Y. Tseng, J. C. Ellenbogen, *Science* **2001**, 294, 1293.
- [9] A. Bachtold, P. Hadley, T. Nakanishi, C. Dekker, *Science* **2001**, 294, 1317.
- [10] P. Avouris, *Acc. Chem. Res.* **2002**, 35, 1026.
- [11] V. Manca, C. Martin-Vide, G. Paum, *BioSystems* **1999**, 52, 47.
- [12] Q. Ouyang, P. D. Kaplan, S. Liu, A. Libhaber, *Science* **1997**, 278, 446.
- [13] L. Wang, Q. Liu, R. M. Corn, A. E. Condon, L. M. Smith, *J. Am. Chem. Soc.* **2000**, 122, 7435.
- [14] M. N. Stojanovic, D. Stefanovic, *Nat. Biotechnol.* **2003**, 21, 1069.
- [15] R. M. Metzger, *Acc. Chem. Res.* **1999**, 32, 950.
- [16] C. Majumder, H. Mizuseki, Y. Kawazoe, *J. Am. Chem. Soc.* **2001**, 123, 9545.
- [17] J. C. Ellenbogen, J. C. Love, *Proc. IEEE* **2000**, 88, 386.
- [18] J. M. Tour, *Chem. Rev.* **1996**, 96, 537.
- [19] J. M. Tour, *Acc. Chem. Res.* **2000**, 33, 791.
- [20] V. Balzani, *Photochem. Photobiol. Sci.* **2003**, 2, 459.
- [21] V. Balzani, A. Credi, F. R. Raymo, J. F. Stoddart, *Angew. Chem.* **2000**, 112, 3486; *Angew. Chem. Int. Ed.* **2000**, 39, 3348.
- [22] V. Balzani, M. Gomez-Lopez, J. F. Stoddart, *Acc. Chem. Res.* **1998**, 31, 405.
- [23] V. Balzani, F. Scandola, *Supramolecular Photochemistry*, Ellies Horwood, New York, **1991**.
- [24] K. Szaciłowski, Z. Stasicka, *Coord. Chem. Rev.* **2002**, 229, 17.
- [25] A. P. de Silva, D. B. Fox, A. J. M. Huxley, T. S. Moody, *Coord. Chem. Rev.* **2000**, 205, 41.
- [26] A. P. de Silva, N. D. McClenaghan, C. P. McCoy, *Handbook of Electron Transfer*, Wiley-VCH, Weinheim, **2000**.
- [27] A. P. de Silva, N. D. McClenaghan, B. O. F. McKinley, M. Querol, *J. Chem. Soc. Dalton Trans.* **2003**, 1902.
- [28] F. R. Raymo, R. J. Alvarado, S. Giordani, M. A. Ceyas, *J. Am. Chem. Soc.* **2003**, 125, 2361.
- [29] F. R. Raymo, S. Giordani, *J. Am. Chem. Soc.* **2001**, 123, 4651.
- [30] F. R. Raymo, S. Giordani, *Org. Lett.* **2001**, 3, 1833.
- [31] F. R. Raymo, S. Giordani, *Org. Lett.* **2001**, 3, 3475.
- [32] F. R. Raymo, S. Giordani, *Proc. Natl. Acad. Sci. USA* **2002**, 99, 4941.

- [33] F. R. Raymo, S. Giordani, *J. Am. Chem. Soc.* **2002**, *124*, 2004.
- [34] F. R. Raymo, S. Giordani, *J. Org. Chem.* **2003**, *68*, 4158.
- [35] A. P. de Silva, Q. N. Gunaratne, T. Gunlasson, A. J. M. Huxley, C. P. McCoy, J. T. Rademacher, T. E. Rice, *Chem. Rev.* **1997**, *97*, 1515.
- [36] F. Pina, M. J. Melo, M. Maestri, P. Passaniti, V. Balzani, *J. Am. Chem. Soc.* **2000**, *122*, 4496.
- [37] O. Steinbock, P. Kettunen, K. Showalter, *J. Phys. Chem.* **1996**, *100*, 18970.
- [38] P. G. Wang, M. Xian, X. Tang, X. Wu, Z. Wen, T. Cai, A. J. Janczuk, *Chem. Rev.* **2002**, *102*, 1091.
- [39] A. R. Butler, I. L. Megson, *Chem. Rev.* **2002**, *102*, 1155.
- [40] V. R. Zhelazkov, D. W. Godwin, *Nitric Oxide* **1998**, *2*, 454.
- [41] G. Stochel, A. Wanat, E. Kuliś, Z. Stasicka, *Coord. Chem. Rev.* **1998**, *171*, 203.
- [42] C. X. Zhang, S. J. Lippard, *Curr. Opin. Chem. Biol.* **2003**, *7*, 481.
- [43] M. Clemente-León, E. Coronado, J. R. Galan-Mascarós, C. J. Gómez-García, T. Woike, J. M. Clemente-Juan, *Inorg. Chem.* **2001**, *40*, 87.
- [44] H. Zhang, J. Cai, X.-L. Feng, H.-Y. Sang, J.-Z. Liu, X.-Y. Li, L.-N. Ji, *Polyhedron* **2002**, *21*, 721.
- [45] Z.-Z. Gu, O. Sato, T. Iyoda, K. Hashimoto, A. Fujishima, *Chem. Mater.* **1997**, *9*, 1092.
- [46] L. V. Zorina, M. Gener, S. S. Khasanov, R. P. Shibaeva, E. Canadell, L. A. Kushch, E. B. Yagubskii, *Synth. Met.* **2002**, *128*, 325.
- [47] K. Ueda, T. Sugimoto, C. Faulmann, P. Cassoux, *Eur. J. Inorg. Chem.* **2003**, 2333.
- [48] M.-E. Sanchez, M.-L. Doublet, C. Faulmann, I. Malfant, P. Cassoux, L. A. Kushch, E. B. Yagubskii, *Eur. J. Inorg. Chem.* **2001**, 2797.
- [49] S. V. Kapelnitsky, E. B. Yagubskii, L. A. Kushcha, I. Y. Shevyakova, *Synth. Met.* **2003**, *133–134*, 443.
- [50] M. Clemente-León, E. Coronado, J. R. Galán-Mascarós, C. Giménez-Saiz, C. J. Gómez-García, J. M. Fabre, G. A. Mousdis, G. C. Papavassiliou, *J. Solid State Chem.* **2002**, *168*, 616.
- [51] K. Szaciłowski, G. Stochel, Z. Stasicka, H. Kisch, *New J. Chem.* **1997**, *21*, 893.
- [52] K. Szaciłowski, A. Wanat, A. Barbieri, E. Wasielewska, M. Witko, G. Stochel, Z. Stasicka, *New J. Chem.* **2002**, *26*, 1495.
- [53] K. Szaciłowski, W. Macyk, G. Stochel, S. Sostero, O. Traverso, Z. Stasicka, *Coord. Chem. Rev.* **2000**, *208*, 277.
- [54] K. Szaciłowski, J. Oszejca, A. Barbieri, A. Karocki, Z. Sojka, S. Sostero, R. Boaretto, Z. Stasicka, *J. Photochem. Photobiol. A* **2001**, *143*, 99.
- [55] K. Szaciłowski, J. Oszejca, G. Stochel, Z. Stasicka, *J. Chem. Soc. Dalton Trans.* **1999**, 2353.
- [56] G. A. Lawrence, M. Maeder, Y.-M. Neuhold, K. Szaciłowski, A. Barbieri, Z. Stasicka, *J. Chem. Soc. Dalton Trans.* **2002**, 3649.
- [57] Y. Marcus, *Ion Solvation*, Wiley, New York, **1985**.
- [58] R. van Eldik, T. Asano, W. L. le Noble, *Chem. Rev.* **1989**, *89*, 549.
- [59] H. Ohtaki, T. Radnai, *Chem. Rev.* **1993**, *93*, 1157.
- [60] Z. Stasicka, E. Wasielewska, *Coord. Chem. Rev.* **1997**, *159*, 271.
- [61] G. Stochel, Z. Stasicka, *Polyhedron* **1985**, *4*, 1887.
- [62] G. Stochel, R. van Eldik, Z. Stasicka, *Inorg. Chem.* **1986**, *25*, 3663.
- [63] S. K. Wolfe, J. H. Swinehart, *Inorg. Chem.* **1975**, *14*, 1049.
- [64] R. van Eldik, W. Gaede, S. Wieland, J. Kraft, M. Spitzer, D. A. Palmer, *Rev. Sci. Instrum.* **1993**, *64*, 1355.

Received: October 28, 2003 [F5663]

Published online: March 22, 2004